

# FATIGUE DAMAGE MECHANISMS IN UNIDIRECTIONAL FIBRE REINFORCED COMPOSITES

LAURA VERGANI

Dipartimento di Meccanica, Politecnico di Milano

## ABSTRACT

With the aim of studying the static and fatigue mechanical characteristics of the pultruded composites, several experimental tests were carried out, by varying the material (in particular the interface fibre-matrix), the grips, the average and amplitude stress values and the stress

great number of applications in particular in USA, but even in other world countries [4].

The pultruded composites are generally constituted by resin matrix and fibre reinforcement and they can weight 50% less than aluminium and 75% less than steel, of equivalent strength.

Fibre content of nearly 85% by weight is possible providing high strength and stiffness in longitudinal direction. Demand for pultrusion is steadily increasing in infrastructure, construction, transportation, consumer, corrosion and electrical markets.

At the moment one of the most interesting application field is represented by the structural profiles, especially for bridge construction and large overhead infrastructure applications.

The initial cost of the pultruded composites is greater (even if the effective cost depends on the production quantity), but over the long run it will be far less expensive, because they will last much longer.

---

## 1. INTRODUCTION

Pultrusion is one of the composite manufacturing process more compatible with low-cost and good-quality requirements of commercial and military production from medium to high-volume one [1, 2, 3].

This process, developed in 1950's, produces high-strength structural composite parts and complex profiles, which are increasingly replacing wood, aluminium and steel in a

Moreover the installation of pultruded composite parts is less expensive, because the beams are so much lighter than steel ones and (for example in civil constructions) a bridge can be pre-assembled into sections and brought to the site of installation. The installation time can reduce from several weeks to a few days.

The pultruded composites are dimensionally stable and do not require maintenance.

Structural pultruded components are replacing steel in off-shore oil exploration and production operations, owing to their weight savings, durability and resistance to salt water and salt air.

In the transportation field it is possible to save 30% weight with a consequent reduction of the consuming and the pollution [5].

Integral composite chassis for truck trailers were realized, thanks to the pultruded characteristics of low weight, corrosion resistance and elimination of painting; in fact pigments added to resin mix provide colour throughout the part.

In the transportation industry the pultruded composites are employed even for roadside structures, that include sign supports, lighting poles and guardrail systems, in fact they are highly-energy absorbent, light-weight and durable.

The process is characterized by low labour content and high raw material conversion for manufacturing profiled shapes at high production rates, attractive cost and consistent quality, without the need for any secondary finishing steps.

The matrix of the conventional pultruded composites is a thermoset resin and the fiber reinforcements are E-glass fibres. Recent processing technology advancements have extended the applicability of the pultrusion process to fibre reinforcements as S-glass, carbon and Kevlar and matrix materials such as thermoplastic.

The pultrusion process is constituted by a number of different phases arranged sequentially and continuously operating. By observing the simple scheme of the pultrusion, shown in Figure 1, it is possible to distinguish in the first step the reinforcing fibre material held on creel racks and continuously fed through a guiding system prior to being impregnated with the specific liquid matrix resin. The fibres impregnated by the resin and preformed by the guiding system into a shape which is similar to the desired finished profile enter the heated curing die. On the die exit the fibres impregnated by the resin have been changed into a fully shaped and solid profile which is gripped by the continuous pulling mechanism at a constant speed. A saw cuts the products to desired length as they approach the end of the line.

The length of an entire pultrusion facility is in order of 10m, but it may be considerably longer if the cross-sections of the pultruded are large and complex.

The process described in Figure 1 is the most basic but also the most common one. In the following the phases which constitute the pultrusion process are described in more detail.

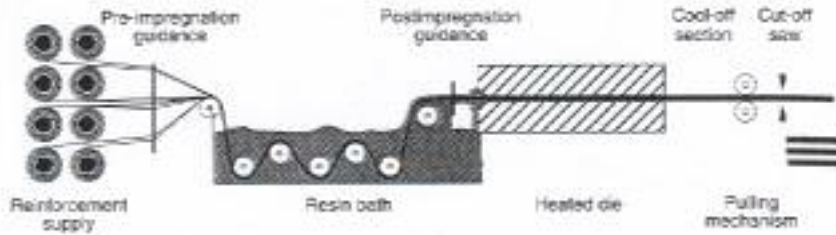


Fig.1: Scheme of the different steps of the pultrusion process

**2. MECHANICAL CHARACTERISTICS**

As previously said, the use of pultruded composites and in general of the advanced reinforced composites is increasing, due to their attractive characteristics.

These composites are expected for applications as structural requiring high durability and reliability.

The definition of the mechanical properties is consequently essential, but due to the heterogeneous structure of these composites which are very complicated since influenced by several factors. In particular it is important to study the fatigue behaviour of these materials, in fact they are sensitive to the cyclic loading, that causes damage and material property degradation.

It is important to accurately evaluate the damage and the degraded properties to ensure that the structures operate with high reliability during their lives. Besides it is

essential to have the tools to predict the performance of the structures in order to schedule the maintenance or replacement of components before failure.

With these aims several experimental tests are planned to investigate the static and fatigue behaviour of pultruded unidirectional fibre composites.

**2.1 Material**

The pultruded composites used for the experimental tests have isoftalic polyester thermoset resin as matrix and E glass as fibres. Their mechanical characteristics are reported in Table 1.

Tab. 1 Mechanical characteristics of matrix and fibres

	Density [g/cm <sup>3</sup> ]	Young modulus [MPa]	Tensile strength [MPa]
Isoftalic polyester	1.28	3,000	55
E glass	2.52	76,000	1,800

Two different composites, called black and white according to their colour, were considered.

They are characterized by the same volume fibre content: 0.65, the same weight fibre content: 0.80 and the same density: 2.05 g/cm<sup>3</sup>. The difference between the two composites is that the black ones have an additive which improves the interfacial adhesion between the resin and E glass fibres and the white ones do not have it [6].

## 2.2 Static mechanical characteristics

The mechanical characteristics of the pultruded composite are strongly influenced by the manufacturing composite process parameters. Different process velocity, different time and temperature of the curing can determine very significant changes in the resulting composite mechanical behaviour. It is possible to define the optimal process parameters to obtain pultruded composites with the best mechanical characteristics.

Besides the mechanical characteristics obtained by means of experimental tests are influenced even by the experimental parameters, as the specimen shape, the grip mechanism, the temperature and the duration of the test. It is possible to define the optimal test parameters to obtain the exact mechanical characteristics corresponding to the composites considered, without external influences.

The mechanical characteristics experimentally found are, therefore, different from the theoretical values that can be defined considering the fibre reinforcement mechanical values by two different effects. The first one depends on the process itself and on the process and product parameters, for instance if the diameter of the pultruded elements is larger, the internal impregnation of the resin results less efficient and, by consequence, the mechanical characteristics will be influenced. The second one depends on the experimental test, in fact some parameters

can strongly influence the experimental test behaviour and the characteristic values.

Several tests were carried out to define the optimal test conditions, that is the conditions to obtain the best results from a group of specimens, from the point of view of mechanical resistance.

The choice of the grips is very important, in fact due to the constant section of the specimen, the gripping specimen zones result more stressed than the central one. The consequence is that the fracture of the specimens is due to the particular grip and it is not a characteristic of the material.

Two types of grips, realized by soft aluminium and pasted to the specimens, were considered in this work[5]. The scheme of the grips, reported in Figure 2, is the same; the differences consist in an internal fillet radius realized as shown in Figure 2.

To evaluate the goodness of the grips and the reliability of the test, the experimental values obtained by the traction tests were compared with the theoretical values obtained by considering the strength and the percent content of glass fibres. An efficiency index is defined:

$$i_s = \frac{S_u}{S_t} \quad (1)$$

where:  $S_u$  is the experimental tensile strength value

$S_t$  is the theoretical tensile strength value.

The  $S_t$  value is easily evaluated:

$$S_t = V_f \cdot S_{rG} = 0.65 \cdot 1800 \text{MPa} = 1170 \text{MPa} \quad (2)$$

where:  $S_{rG}$  is tensile strength value of the E glass (see Table 1)

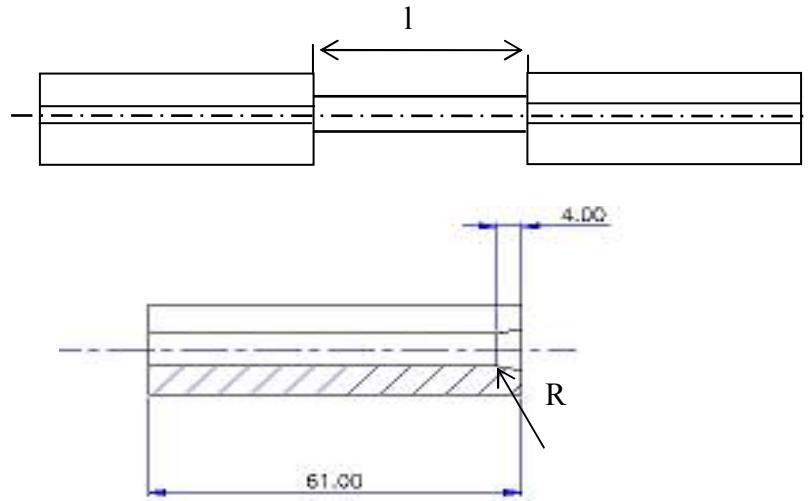


Fig.2 Soft aluminium grips: there is a type without the fillet radius and a type with the internal fillet radius R

It is possible to define an efficiency coefficient by evaluating the experimental elastic modulus E and by comparing it with a theoretical one, evaluated by the simple mixture rule:

$$i_E = \frac{E}{E_t} \quad (3)$$

where: E is the experimental tensile elongation modulus  
 $E_t$  is the theoretical tensile elongation modulus

It is possible to define:

$$E_t = V_m E_m + V_f E_f \quad (4)$$

Where:  $E_m$  and  $E_f$  are the elastic modulus respectively of the matrix and the fibres  
 $V_m$  and  $V_f$  are the volumetric fraction respectively of the matrix and the fibres

By the values of Table 1:

$$E_t = 0.35 \cdot 3,000 + 0.65 \cdot 76,000 = 50,450 \text{ MPa}$$

### 3. EXPERIMENTAL TESTS

#### 3.1 Tensile tests

Several tensile tests were carried out in order to determine the material strength values not dependent on experimental test conditions. The test machine is an electromechanical MTS with maximum load 100 kN.

The tests were carried out under displacement control.

Specimens with a diameter  $d=6\text{mm}$  and a useful length  $l=50\text{mm}$  were used.

The strains were measured by means of an axial extensometer MTS with a base length equal to 25 mm.

The average experimental values found by the white and the black specimens by using the different grips were shown in table 2.

From the values of Table 2 it is evident that there are not significant differences relating to the tensile behaviour of the black and the white specimens.

**Tab. 2: Tensile strength experimental values**

	$S_u$ [MPa] Tensile strength	$\epsilon_u$ [%] fracture strain	E [MPa] Elastic modulus
<b>Black specimens</b> Grips without fillet radius	884±15	2.1±0.1	43,240± 1400
<b>Black specimens</b> Grips with fillet radius	1015±50	2.5±0.3	44,330±1500
<b>White specimens</b> Grips without fillet radius	886±20	2.0±0.1	47,170±1700
<b>White specimens</b> Grips with fillet radius	987±30	2.2±0.2	46,090±1700

The stress-strain curves show a linear behaviour of the material till the fracture.

The index  $i$ , evaluated by considering the values of theoretical and experimental strengths and by considering the highest values obtained by means of the grips with fillet radius, for the black specimens results:

$$i_s = \frac{S_u}{S_t} = \frac{1015}{1170} = 0.87$$

for the white specimens:

$$i_s = \frac{S_u}{S_t} = \frac{987}{1170} = 0.84$$

and by the values of the elastic modulus, for the black specimens:

$$i_E = \frac{E_e}{E_t} = 0.88$$

and for the white specimens:

$$i_E = \frac{E_e}{E_t} = 0.91$$

Several tests were carried out by varying the internal fillet radius with the aim to improve the strength values, but no further improvement was obtained.

It is possible to say that the test conditions are optimal and the differences with the theoretical value are due to the material defects.

The values of the indexes obtained by the black and the white specimens are similar, due to the fact that the tensile characteristics are not particularly influenced by the interfacial bonding.

The aspect of the static fracture is shown in Figure 3.



Fig.3a: Black specimen fractured

Fig.3b: White specimen fractured

### 3.2 Compression tests

The specimens used to perform the compression tests are similar to the ones used for the

tensile tests except for the length, in fact to avoid problem of elastic instability the specimen useful length between the grips is lower, in particular  $l=20\text{mm}$ .

The test machine is the same used for the tensile test. The strains were measured by an extensometer MTS with a base length equal to 8mm.

Several tests were carried out and the results are shown in Table 3.

Tab. 3: Compression strength experimental values

	$S_{uc}$ [MPa] Tensile strength	$\epsilon_{uc}$ [%] fracture strain	E [MPa] Elastic modulus
Black specimens	1050±50	2.5±0.2	45,000 ± 1700
White specimens	600±30	1.3±0.1	50,000±2400

The efficiency coefficient is defined even in the case of the compression tests; the values found are for the black specimens (grips with internal fillet radius):

$$i_{s,c} = \frac{S_{uc}}{S_t} = \frac{1050}{1170} = 0.90$$

and for the white specimens (grips with internal fillet radius):

$$i_{s,c} = \frac{S_{uc}}{S_t} = \frac{600}{1170} = 0.51$$

The different behaviour between the black specimens, that have a special additive to

improve the interface adhesion, and the white ones, that do not have the additive is evident. In particular the tensile values (see Table 2) are not influenced by the presence of the additive, on the contrary the compression strength values are greatly dependent on the interfacial bonds.

#### 4. MICROSCOPIC EXAMINATION

In order to understand the behaviour of the specimens statically loaded and to evidence the material damage mechanism, several analyses were carried out by means of a scanning electronic microscope.

##### 4.1 Microscopic examination in the material not loaded

Different defect types are present in the specimens before they are loaded. The alignment of the fibres is not always respected, as it is evident in Figure 4a, where there are fibre groups not well lined up. The density of the fibres is not uniform, as Figure 4b shows: in some zones there are more fibres than in others. Other typical defects are the presence of fractured fibres and cracks in the matrix.

All these defects justify the difference between the strength values experimentally found and the theoretical ones.

With the aim to follow the mechanism damage in the material during the tensile and the compression tests, several microscopic analyses were performed by interrupting the test at a fixed percentage of the strength value. The

specimens were cut and observed by a scanning electron microscope. By always considering the same enlargement (50X), the number and the dimensions of three different defects (matrix cracks, fibre cracks, interface cracks) were measured.

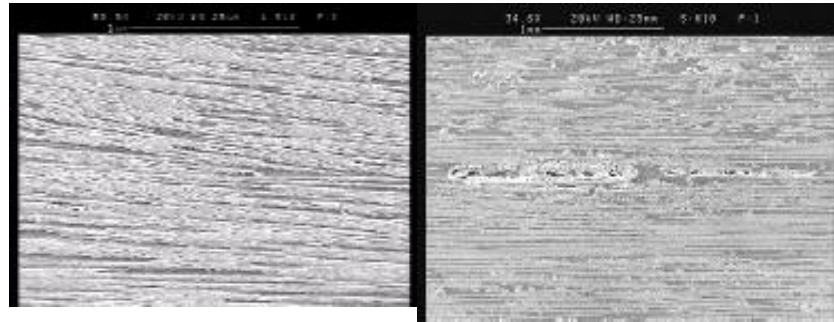


Fig.4a: Magnification 50x shows fibres not lined up in the specimen  
 Fig. 4b: Magnification 35x shows different fibre density in the specimen

#### 4.2 Black specimens

Several tensile tests were interrupted at different percentage of the strength value, in particular in correspondence of the following values:  $\sigma/S_u=0.13, 0.24, 0.41, 0.66$ . All the specimens were cut and examined by the scanning electronic microscope.

The damage evolution was associated with the number and the type of the defects, by always considering the same enlargement and consequently the same area of material. It is possible to note that with the load increasing

the number of the fibre fractured greatly increases, on the contrary the other defect types (the matrix and interface cracks) are not rising with the same proportion.

In Figure 5a the enlargement of the section cut from the specimen loaded till the  $\sigma/S_u=0.24$  value is shown and in Figure 5b the enlargement corresponding at a specimen loaded till the  $\sigma/S_u=0.66$  is shown too. The comparison is evident: in the first one the number of fibres fractured is about 10 and in the second one is about 30 over the same section.



Fig.5a: Enlargement of a section of the specimen loaded until  $\sigma/S_u=0.24$ . Number of fibre cracks is about 10; number of matrix cracks is about 4, number of interface cracks is about 1, with length 0.35mm  
 Fig.5b Enlargement of a section of the specimen loaded until  $\sigma/S_u=0.66$ . Number of fibre cracks is about 30; number of matrix cracks is about 1, number of interface cracks is about 5, with length 0.35mm

In Figure 6 the number of the different defects is shown with respect to the loading applied. It is evident that during the traction tests the damage evolution consists in an increasing of

the cracked fibres, on the contrary it is not possible to note an evolution of the other defects.

The interface crack length was measured too, but, as it is possible to see in Figure 6b, there is not an evident correlation between the loading increase and the crack length.

Similar observations carried out from the white specimens put in evidence the same behaviour even if a larger number of defects at the interface was detected.

### 4.3 Compression tests

Different compression tests were interrupted in order to examine the internal damage by the electronic microscope.

Black specimens compression tests were interrupted in correspondence of  $\sigma/S_u=0.13$ ,  $0.35$ . The number of the defects is lower with respect to the traction tests, but the cracks in the matrix are larger and placed along the longitudinal direction.

The observations carried out by the white specimens resulted significantly different. In fact, as it is shown in Figure 7, there is a larger number of defects and in particular of interface cracks.

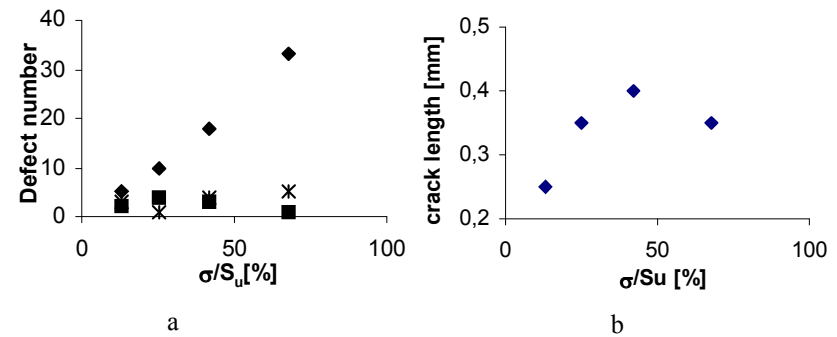


Fig.6: Traction test: evolution of the defects in the black specimens with respect to the loading applied; a) number of the defects: ♦ fibre cracks; \* matrix cracks; ■ interface cracks; b) length of the crack at the interface between matrix and fibres.

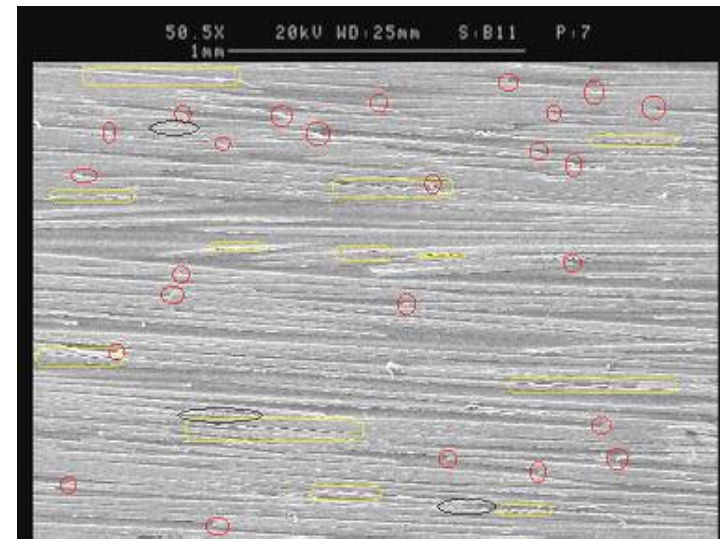


Fig.7 Enlargement of a section of a white specimen loaded until  $\sigma/S_u=0.26$ .

By these observations the damage evolution during traction tests seems to be different than during a compression tests. When a traction loading is applied, the principal damage consists in a progressive fracture of the fibres, that it is not influenced by the interface behaviour. In fact the black and the white specimens that are characterized by different interface conditions, due to the presence of an additive in black specimens, show similar trends during the traction tests as it is reported in Table 2.

Different values are, on the contrary, found when a compression load is applied. In fact in this case the interface bonding plays an important role and, as it is reported in Table 3, influences the fracture values in a significant way.

## 5. FATIGUE TESTS

Several axial fatigue tests were carried out by varying the amplitude and the average of the load applied, the frequency and the external temperature.

The fatigue tests were stopped in correspondence of the rupture of the specimens or after  $4 \cdot 10^6$  loading cycle without damage of the specimen.

Different fracture ways were verified. The results, which were considered valid are related to the specimens where the damage begins far from the grips. In these cases the appearance of the specimen is as in Figure 8.

The specimens used are the ones shown in Figure 3 (diameter  $d=6\text{mm}$ , useful length  $l=50\text{mm}$ ). The test machine is an hydraulic MTS with maximum load 100 kN.



*Fig.8: Typical appearance as brush of a fractured specimen*

Fatigue tests are carried out under load control conditions. The fatigue load is applied in a sinusoidal form.

All the first series of tests are performed in ambient temperature. The frequency is maintained constant and  $f=5\text{Hz}$ . In the second series of tests the parameters that were changed are the external temperature and the frequency.

An extensometer MTS was located across the central part of the specimens and, at regular intervals during the fatigue testing, a slower cycle was incorporated so that the values of load-displacement could be recorded. These data allow to evaluate the stress-strain values.

At the end of the tests the collected data were analysed in order to define the variations of the stress-strain curves and in particular of the elastic modulus,  $E$ , during the specimen life.

To study the different types of damage and their evolution during the fatigue tests, samples were removed at a fixed fractions ( $N/N_f$ ) of the

predicted lifetime  $N_f$ . These samples were cut and examined by using a scansion electronic microscope.

**5.1 Effect of the stress ratio and of the gripping conditions**

Several tests were carried out, by means of the black and the white specimens, by varying the average and the amplitude stress values and the stress ratio R, in particular R=-1, 0.1, 0.3 and 0.5.

The grip conditions were varied too, by considering grips with and without internal fillet, as shown in Figure 2.

All the results obtained from the fatigue experiments, carried out by the black and the white specimens, are shown in Table 4 and 5 and in Figures 9 and 10.

The white specimens fatigue tested seemed more sensitive to the gripping conditions, in fact it was possible to perform the fatigue tests only with the grips with internal fillet radius.

In order to investigate the effect of the average on the amplitude stress, the black specimens with the grips without fillet radius are considered. The amplitude values are shown in Figure 10, where the linear interpolations, in correspondence of the different stress value ratios R, are evidenced.

From this diagram it is evident that by increasing the average stress value the life corresponding to a particular amplitude decreases [7-11].

Tab.4: Fatigue experimental results from black specimens with grips without fillet radius

R=-1		R=0.1		R=0.3		R=0.5	
$S_{max}$ [Mpa]	$N_f$	$S_{max}$ [Mpa]	$N_f$	$S_{max}$ [Mpa]	$N_f$	$S_{max}$ [Mpa]	$N_f$
350	1664	613	300	630	950	720,0	1016
350	710	500	2495	580	2307	540,0	6450
350	812	450	6170	514	2980	500,0	8100
325	4685	400	15820	450	6000	450,0	14550
325	11080	350	21725	386	26625	400,0	41725
325	5127	300	75625	346	30830	350,0	228005
300	11526	250	377500	321	66485	333,3	276138
300	5695	222	1668525	296	150505	300,0	478480
300	5312	200	No bro.	250	377000	250,0	no bro
275	17615			214	no bro		
275	19082						
275	13388						
250	19426						
250	63583						
250	37520						
225	144152						
200	205802						
180	449042						
180	388636						
180	2870402						
130	no broken						

The relation between the stress amplitude and the life  $N_f$  is:

$$S_a = AN_f^m \tag{5}$$

where m is about constant and A is dependent on R.

Tab. 5: Fatigue experimental results from black and white specimens with grips with internal fillet radius

R=0.3			
Black specimens		White specimens	
$S_{max}$ [Mpa]	$N_f$	$S_{max}$ [Mpa]	$N_f$
714	1468	630	710
630	3820	580	519
580	4100	514,2	1250
514	14700	450	3008
386	60400	385,7	43000
321	415359	346,1	208600
286	449405	321,4	51986
286	15445612	285,7	747500
250	Not broken		
250	Not broken		

From the experimental values it is possible to define the different R values considered:

$$R=-1 \quad S_a = 780(N_f)^{-0.110} \quad R^2=0,930$$

$$R=0.1 \quad S_a = 570(N_f)^{-0.123} \quad R^2=0,988$$

$$R=0.3 \quad S_a = 540(N_f)^{-0.137} \quad R^2=0,970$$

$$R=0.5 \quad S_a = 390(N_f)^{-0.125} \quad R^2=0,979$$

The dependence of A on R values is evidenced by the diagram of Figure 11. By means of a linear interpolation of the data the following relation is found:

$$A = 564 - 227R \quad R^2=0.923$$

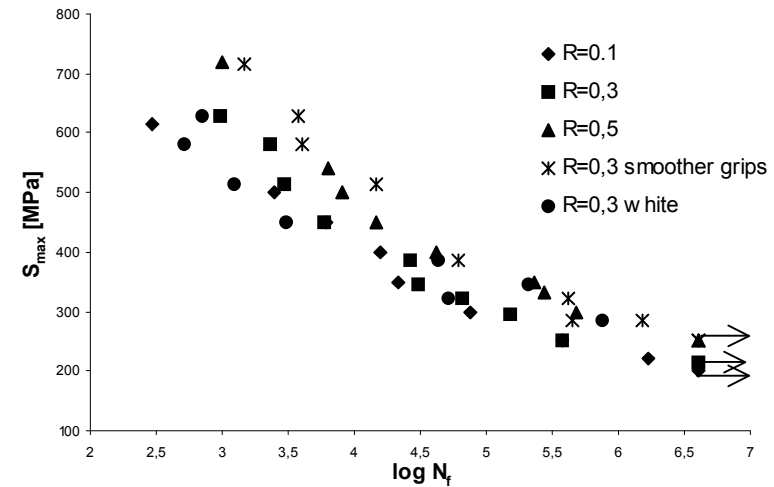


Fig.9: Maximum stress versus the fatigue life of all the specimens (except R=-1) (→:specimen not broken)

To put in evidence the effect of the mean stress constant life curves, the Goodman diagrams, can be used. The trend that is determined is linear, as it is possible to see in Figure 12, where the curves in correspondence of  $N_f=10^4$ ,  $10^5$ ,  $10^6$  number of loading cycles are represented.

In order to define the effect of the grips, the results from black specimens at R=0.3 are compared in Figure 13.

From this diagram the improvement due to the smoother gripping is evident, in fact the fatigue performance of the black specimens increases of about the 30% by using these grips. By the same gripping conditions the fatigue limit was experimentally found by means of Dixon method. The value of the stress amplitude

determined is:  $\sigma_{Fa}=93$  MPa with an average value  $\sigma_m=173$  MPa, corresponding to a stress ratio  $R=0.3$ .

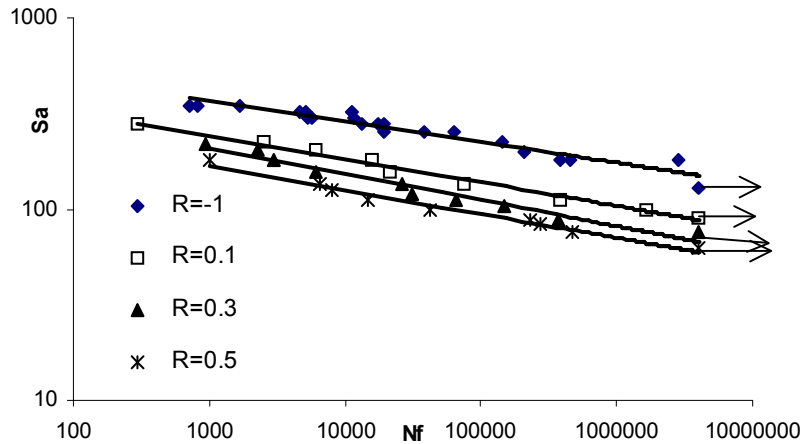


Fig.10: Trend of the stress amplitude with respect to the number of loading cycles and the stress ratio  $R$  (black specimens and grips without fillet radius);  $\rightarrow$  specimen not broken

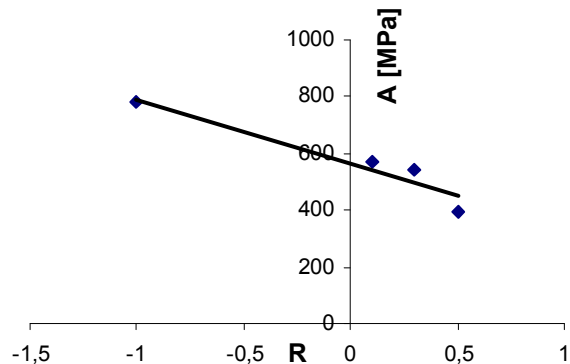


Fig.11: Coefficient  $A$  with respect to  $R$  values

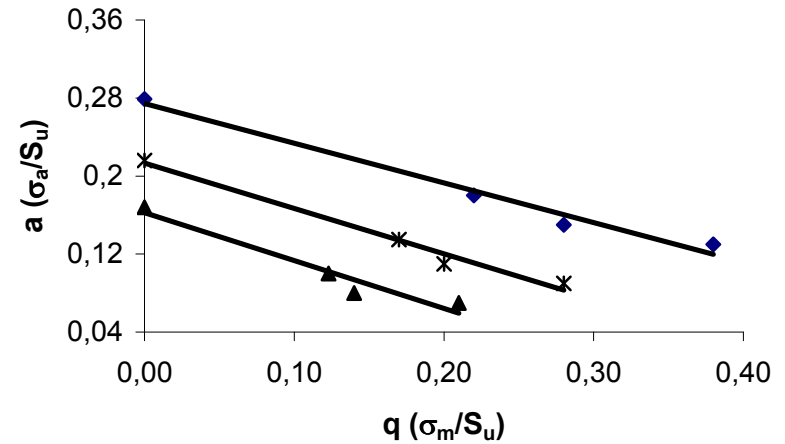


Fig.12 Effect of the mean stress: non dimensional curves at constant life  
 (---♦---  $N_f=10^4$ ; ----\*---  $N_f=10^5$ ;  $N_f=10^6$  --▲----)

The white specimens fatigue results are reported in Figure 14. The fatigue tests were carried out by using the grips with internal fillet radius, in fact it was not possible to perform these test series with the other grips, due to the damaging of the white specimens in the grip zones. The tests were effectuated by a stress ratio  $R=0.3$ . The results compared with the corresponding ones, obtained by the black specimens, were shown in Figure 14.



-specimen geometry as in Figure 2

The parameters that are changed are:

- temperature 20°C and 50°C
- frequency 5Hz and 15Hz

The tests carried out and the results obtained are shown in Table 6. All the hypothesis of the variance analyses are verified. The tests of normality and homogeneity are satisfied. The data elaborated show that the temperature is a significant parameter, on the contrary the frequency is less significant.

Tab. 6: factorial plane of the experimental tests

	f=5Hz		f=15Hz	
	N° test	N <sub>f</sub>	N° test	N <sub>f</sub>
T=20°C	1a	71264	1b	54481
	2a	110291	2b	93154
	3a	184807	3b	60589
T=50°C	1c	13028	1d	21991
	2c	20397	2d	34575
	3c	17668	3d	17494

## 6. FATIGUE DAMAGE

Fatigue of fibre reinforced composite materials is a quite complex phenomenon. Composite materials are inhomogeneous and anisotropic and their behaviour is more complicated than the corresponding one of homogeneous and isotropic materials as the metals.

Under cyclic loading the damage will accumulate in composite materials characterized by multiple damage modes, such as cracking of the matrix, fibre-matrix decohesion, fibre fracture. Even for unidirectional reinforced composites under the tension loading along the fibre direction, cracks can initiate at different locations and in different directions.

On the other hand, for homogeneous and isotropic materials damage is accumulated at a low growth rate in the beginning and a single crack propagates in a direction that is perpendicular to the cyclic loading axis.

As a consequence of this complexity and variety of damage modes no theories have been developed that are capable of accurately predicting the general failure process.

In literature it is possible to find several fatigue criteria suitable for composite materials. In [12] the criteria are classified in three principal groups: a) fatigue life models, which do not consider the effective damage of the material and are based on S-N curves [13-16]; b) phenomenological models, that consider the evolution of the damage in terms of macroscopically observable properties, as the residual strength and the residual stiffness. In particular residual stiffness measurement does not involve destruction of the test specimen and can be measured easily and frequently during the fatigue experiments [17, 18]. This model may be deterministic, in which a single-valued stiffness property is predicted or statistical, in which predictions are for stiffness or strength distribution [19]; c) criteria based on

the progressive damage models, which consider one or more damage variables related to measurable manifestation of damage, as number of cracks, debonding size [20, 21, 22].

### 6.1 Stiffness measurements

In this work the stiffness was measured during the fatigue experiments.

The material considered has a high percentage of glass fibre and its global behaviour is fibre-dominated, in fact the trend, in terms of stress-strain during the tensile tests, is linear till the fracture, and the cycles measured during the fatigue tests are always linear without hysteretic phenomenon.

The fatigue damage was measured in term of elastic modulus  $E$  divided by  $E_0$  that is the value measured during the first loading cycle. The trend found is similar to the ones reported in [ 9, 10].

As it is shown in Figure 15, which describes the comparison between the stiffness values, measured by two specimens subjected to different values of maximum stress and the same stress ratio, in the trend of the normalized elasticity modulus, it is possible to distinguish three regions.

The first region is localized at the beginning of the test and corresponds to a sudden drop of the values. This phase is quite always detectable in the fatigue tests, but it was not possible to correlate it with the stress values, in fact the drop amplitude seems to be not dependent on this value. In the figure it is possible to see this phase only in the

curve carried out by the specimen subjected to a lower load (continuous line).

The second phase consists in a more gradual decrease of the normalized elastic modulus. Some times in this phase two different slopes are easily visible: the first is lower than the second one, due to a lower damage velocity.

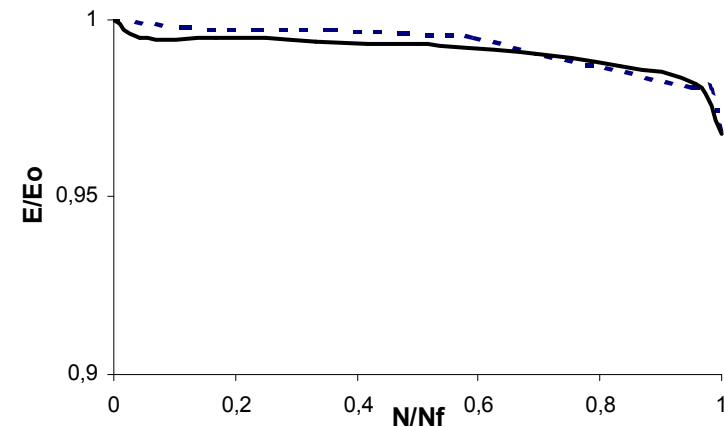


Fig. 15 Comparison between the trend of the normalized elastic modulus by two different black specimens loaded by different values of the maximum stress (with the grips with internal fillet radius: ---  $S_{max}=400\text{MPa}$ ,  $R=0.1$ ,  $N_f=16,000$ ; —  $S_{max}=350\text{MPa}$ ,  $R=0.1$ ,  $N_f=24,000$ ).

After a decrease of about 2-4% of  $E/E_0$  the final phase begins corresponding to a very rapid damaging of the specimen that presents a fracture as brush, see Fig 8.

The decrease value of the normalized elastic modulus is always low, if compared to the other

ones found in literature. This is probably due to the high percentage of glass fibre present and to the strong interface bond between the matrix and the glass. In fact the trends of  $E/E_0$  values showed by the white specimens, which have a less stronger interface bond, present higher decrease values, as it is visible in Figure 16.

The curve presented in this figure has the same characteristics of the black specimens, even if the values decrease is larger.

However the measurements of the elastic modulus resulted often difficult and the values not always reliable, in fact the strain values measured by the extensometer depend on the local position of the knives of the extensometer, due to the internal debonding that causes the composite to elongate along different fibre bundles.

In order to obtain a damage accumulation curve, the definition of damage reported in [23] is used:

$$D^* = \frac{E_0 - E}{E_0 - E_f} \quad (6)$$

where  $E_f$  is the elastic modulus measured in correspondence to the fracture.

Several  $D^*$  curves were obtained by corresponding to the different fatigue tests. The scattering of the damage curve trends results elevated.

An average curve found from the results of the black specimens is compared with the corresponding curve determined from the white specimens in Figure 17.

From this comparison it is evident that the white specimens present a larger damaging during the fatigue tests, as already evidenced in terms of stiffness.

It is possible to verify that the ratio between the  $D^*$  values obtained by the white and the black specimens, in the central zone of the diagram of Figure 17, is almost equal to the ratio between the efficiency coefficient obtained by means of the compression tests.

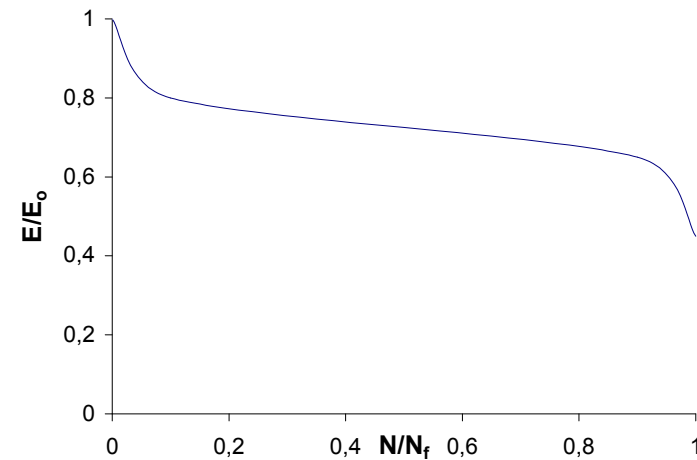


Fig. 16 Normalized elastic modulus trend of a white specimen:  $S_{max}=346$ ,  $R=0.3$ ,  $N_f=208,000$ .

## 6.2 Microscopical damage

The fatigue tests were interrupted at some intervals of the specimen life in order to cut the specimens and observe by the scanning

electronic microscope the internal damage of the composites. Three different damage types were individuated: fibre cracks, matrix cracks and debonding between the fibre and the matrix. To consider the evolution of the first two types the number of the cracks was evaluated, on the contrary the evolution of the third damage type was considered in terms of length of the crack between the matrix and the fibres.

The evolution of the damage was evaluated by means of black and white specimens by varying even the gripping modes.

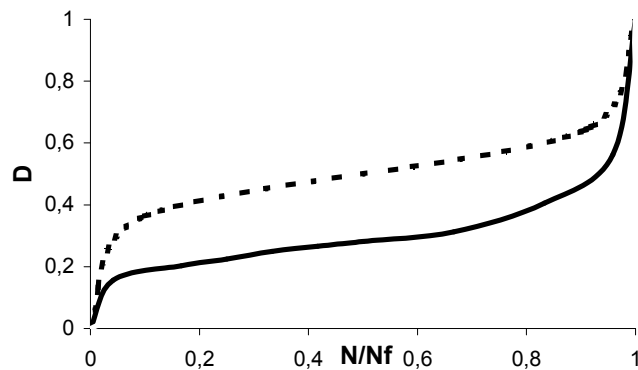


Fig.17: Damage curves: —black specimens; ----- white specimens.

The evolution of the damage resulted almost the same for all the specimens: in the first phase, which ends in correspondence to about 2% of  $N_f$ , the formation of defects is

detected, on the contrary in the second phase the growth of the previously created defects is generally detected.

This behaviour is common to the different specimens, black and white, and to the different testing conditions.

The influence of the stress values was in particular investigated. Several tests on black specimens were effectuated, by maintaining  $R=0.1$  and varying the stress amplitudes. All the tests were performed with the improved gripping conditions. Three different series of tests were performed with the following maximum stress values  $S_{max}=500, 350, 250$  MPa.

By considering as  $N_f$  value the one previously found by the experimental fatigue, see Table 4, the tests were interrupted at about the same life percentages.

The specimens were cut and analysed by the electron scanning microscope, by considering the same enlargements the fibre cracks were counted. Each value of defect number reported in Figure 18 is an average value obtained by three measurements effectuated on the same surface extension of three different specimens.

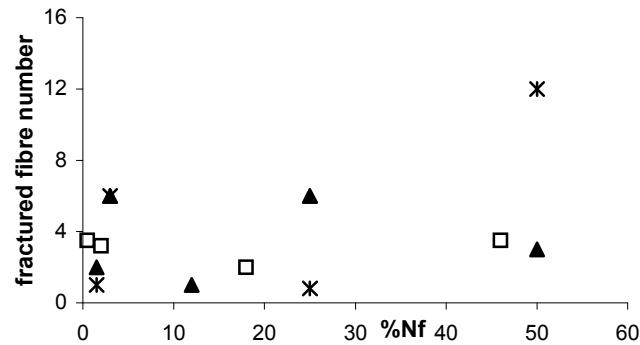


Fig.18 Number of fractured fibres  $R=0,1$ : \*  $S_{max}=500\text{MPa}$ ; □  $S_{max}=350\text{MPa}$ ; ▲  $S_{max}=250\text{MPa}$

By observing the Figure 18 it is difficult to define a trend of the number of fibre fractured with respect to the fatigue life. It seems that the number of fibre cracks remains substantially constant after the first phase and that is almost directly depending on the value of the maximum stress applied.

A similar result is obtained if the number of matrix cracks is considered.

By the SEM observations the length of the crack at the interface between the fibres and the matrix was measured too, as it is shown in Figure 19.

From this diagram it is evident that the length of interface crack is increasing with the specimen life, after a first step till 2-3%  $N_f$ .

Moreover the length values are depending on the effective number of loading cycle; in fact the largest lengths are related to the lowest

stresses applied values and longest lives, on the contrary the smallest cracks are related to the largest stresses and shortest lives.

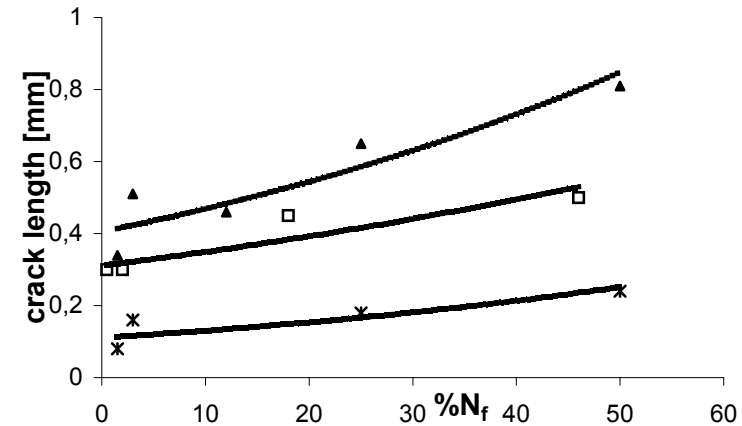


Fig.19 Interface crack length measured by black specimens:  $R=0,1$ ; \*  $S_{max}=500\text{MPa}$ ; □  $S_{max}=350\text{MPa}$ ; ▲  $S_{max}=250\text{MPa}$

Some other comparisons were carried out by considering the microscopic behaviour of the white specimens and of the black specimens. The evolution of the number of the interface cracks is compared in Figure 20.

## 7. CONCLUSIONS

Several experimental tests were carried out with the aim to investigate the static and fatigue behaviour of the unidirectional reinforced pultruded composites.

The following conclusions are pointed out:

-The testing conditions greatly influence the experimental results. It is necessary to optimise the testing parameters, in terms of specimen geometry, grippings, gripping pressure, in order to obtain experimental results not dependent on these;  
It was verified that grippings with an internal fillet radius improve the fatigue results.

-Mechanical characteristics are influenced by the interfacial bonds, in particular the effect is consistent when compression or variable loadings are applied, on the contrary the tensile characteristics are not dependent on this parameter in a significant way;  
-the fatigue trend is satisfactorily described by the relation:  $S_a = A \cdot N_f^m$

where the exponent m is almost constant if stress ratio R changes, on the contrary the coefficient A is dependent on R.  
The composites with a lower interfacial bond are less resistant to the variable loadings, presenting a lower fatigue life, and the experimental results are more scattered;  
-scansion electron microscope measurements show that during the application of the tensile loadings the damage is constituted by the fracture of the fibres and of the matrix and the number of the cracks in the fibres and in the matrix is directly dependent on the load level.  
During the first phase of the fatigue testing (till about the 2% of  $N_f$ ) the damage consists in the breaking of fibres, matrix and of the

interfacial bond between the matrix and the fibres, in the second phase of the fatigue life, on the contrary, the damage consists in the propagation of the interfacial cracks. It was found that the length of interfacial cracks is dependent on the number of loading cycles and not on the stress applied amplitude. In particular the longest crack are corresponding to the lowest stress amplitude;

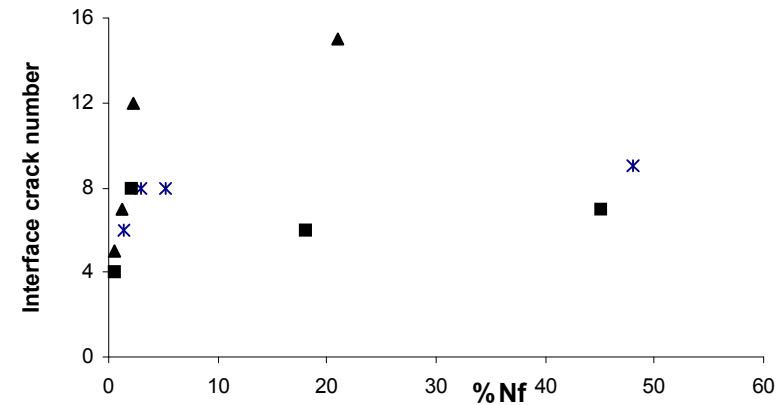


Fig. 20 Evolution of the number of the interface cracks during the specimen life: ▲ white specimens; ■ black specimens with connection; \* black specimens without connection

-the value of the elastic modulus measured during the fatigue tests is not an efficient damage parameter, in fact, the fatigue damaging consists in the propagation of the interfacial cracks, that do not greatly influence the tensile characteristics;

-the ANOVA approach was followed to study the influence of the external temperature and of the frequency: the statistical elaboration of the experimental results evidences a strong influence of temperature and not of frequency.

## 8. ACKNOWLEDGEMENT

The author would like to thank PLACO S.R.L for the supply of all the specimens.

## 9. REFERENCES

1. Trevor F. Starr (ed) *Pultrusion for Engineers*, CRC Press, Woodhead Publishing limited, Cambridge, England, 2000.
2. Åström B. T. *Manufacturing of Polymer Composites*, Chapman & Hall, London, UK, 1997.
3. Fanucci J. and al., *Pultrusion of Composites Advanced Composites Manufacturing*, Chapter 7, ed. T.G. Gutowski, J.Wiley & Sons, Printed in USA, pp.259-295, 1997.
4. Edwards K.L., An overview of fibre reinforced plastics for design purposes, *Material and Design*, N.19, 1998.
5. Donti R., Vaughan V., Fatigue testing of Pultruded Composite Materials, *Experimental Techniques*, may/june 1994, pp.27-29
6. Koichi G., The role of interfacial debonding in increasing the strength and reliability of unidirectional fibrous composites, *Composites Science and Tecnology*, 59, 1999.
7. Demers Cornelia E., Tension-tension axial fatigue of E-glass fibre-reinforced polymeric composites: fatigue life diagram, *Construction and Building Materials*, 12, pp.303-310, 1998.
8. Demers Cornelia, Fatigue strength degradation of E-glass FRP composites and carbon FRP composite, *Construction and Building Materials*, 12, pp.311-318, 1998.
9. Demers Cornelia, Tension-tension axial fatigue of E-glass fiber-reinforced polymeric composites: tensile fatigue modulus, *Construction and Building Materials*, 12, pp.51-58, 1998.
10. Moura Branco C., Ferreira J. A. M., Costa J.D.M., Richardson M.O.W., A comparative study of the fatigue behaviour of GRP hand lay-up and pultruded phenolic composites, *International Journal of Fatigue*, 18, N°4, pp.255-263, 1995.
11. Ferreira J. A. M., Costa J.D.M., Richardson M.O.W., Effect of notch and test conditions on the fatigue of glass-fibre reinforced polypropylene composite, *Composite Science and Technologies*, 57, pp. 1243-1248, 1997.
12. Degrieck J., Van Paepegem W., Fatigue Damage Modelling of Fibre-reinforced Composite Materials: Review, *Applied Mechanics Reviews*, 54(4), pp.279-300, 2001.
13. Shokrieh M.S., Lessard L.B., Multiaxial fatigue behaviour of unidirectional plies based on uniaxial fatigue experiments, *International journal of fatigue*, Vol.19, N°3, pp. 210-207, 1997.
14. Plumtree A., Shen G., Prediction of Fatigue Damage Development in Unidirectional Long

- fibre Composites, *Polymers and Polymer Composites*, Vol 2, No. 2 ,1994.
- 15.Plumtree A., Cheng G.X., Fatigue damage parameter for off-axis unidirectional fibre-reinforced composites, *International Journal of fatigue*, 21, 1999.
  - 16.Petermann J., Plumtree A., A unified fatigue failure criterion for unidirectional laminates, *Composites : Part A*, 32 , 2001.
  - 17.Whitworth H.A., A Stiffness Degradation Model for Composite Laminates under Fatigue Loading, *Composite Structures*, Vol.40, N°2, pp.95-101, 1998.
  - 18.Dyer K.P., Isaac D.H., Fatigue behaviour of continuous glass fibre reinforced composites, *Composites Part B*, 49B, pp.725-733, 1998.
  - 19.Caprino G., Giorleo G., Fatigue lifetime of glass fabric/epoxy composites, *Composites: part A*, 30, pp.299-304, 1999.
  - 20.Plumtree A., Shi L., Fatigue damage evolution in off-axis unidirectional CFRP, *International Journal of Fatigue*, 24 , 2002.
  - 21.Reifsnider K., Case S., Duthoit J., The mechanics of composite strength evolution, *Composites Science and Technology*, 60, pp. 2539-2546, 2000.
  - 22.Subramanian S., Reifsnider K., Stinchcomb W.W., A cumulative damage model to predict the fatigue life of composite laminates including the effect of a fibre-matrix interphase, *International J. of fatigue*, Vol. 17, N°5, pp.343-351, 1995.
  - 23.Mao H., Mahadevan S., Fatigue damage modelling of composite materials, *Composites structures*, N°58, pp.405-410, 2002.